

JOPAT Vol 23(1) 1293– 1312, Jan – June. 2024 Edition.

ISSN2636 – 5448 <https://dx.doi.org/10.4314/jopat.v23i1.8>**Integrated Approach for studying Anti-angiotensin Converting Enzyme activity of Triazole Derivatives to Down-regulate Diabetes**Oyebamiji Abel K. <sup>1,8\*</sup>, Akintelu Sunday A.<sup>2</sup>, Akintayo Emmanuel T.<sup>3</sup>, Akintayo Cecilia O. <sup>4</sup>, Ebenezer Oluwakemi<sup>5</sup>, Ogunlakin Akingbolabo Daniel<sup>6,8</sup>, Ojo Oluwafemi Adeleke<sup>6,8</sup>, Babalola Jonathan O. <sup>1,7,8</sup><sup>1</sup>Industrial Chemistry Programme, Bowen University, PMB 284, Iwo, Osun State, Nigeria.<sup>2</sup>School of Chemistry and Chemical Engineering, Beijing Institute of Technology, Beijing 100811, China.<sup>3</sup>Department of Chemistry, Ekiti State University, Ado-Ekiti, Nigeria.<sup>4</sup>Department of Chemistry, Federal University, Oye-Ekiti, Nigeria.<sup>5</sup>Department of Physics, University of Alberta, Edmonton, AB T6G 2E1, Canada.<sup>6</sup>Biochemistry Programme, Bowen University, Iwo 232101, Nigeria.<sup>7</sup>Department of Chemistry, University of Ibadan, Ibadan, Nigeria.<sup>8</sup>Good Health and Wellbeing Research Clusters (SDG 03), Bowen University, Iwo 232101, Nigeria.**Abstract:**

The effects of triazole and its derivatives as anti-angiotensin converting enzyme activity were investigated using combined computational approach. This work is directed at examining the anti-angiotensin converting enzyme activity of the studied triazole derivatives via density functional theory and molecular modeling studies using *in silico* approach. This work was executed using Spartan 14 for optimization. The downloaded receptor (human angiotensin-converting enzyme (PDB ID: 3NXQ)) from protein data bank by removing water molecules and other small molecules downloaded with the target before subjecting it to docking calculation and molecular dynamic simulation studies. In this work, we discovered that addition of methyl and 2-ethyl-1*H*-indole to triazole as parent compound enhanced the activity of compound **4** and this was revealed via the predicted highest occupied molecular orbital (HOMO) (-4.53 eV) and energy gap (3.73 eV). More so, Compound **4** with -10.5 kcal/mol possess the highest strength to impede human angiotensin-converting enzyme (PDB ID: 3NXQ) than other investigated compound and the metformin. The developed quantitative structure activity relationship (QSAR) with squared correlation coefficient ( $R^2$ ) of 0.745234 and adjusted  $R^2$  of 0.617852 proved to be valid and predictable which was confirmed via the predicted percentage inhibiting concentration (% $IC_{50}$ ). The molecular dynamic simulation and pharmacokinetic studies of the compound ((Compound **4**) and the reference drug (metformin)) that possess the highest binding affinity were investigated and reported. These findings may give insight into developing library of drug-like triazole-based compounds as proficient anti-diabetic agents.

**Keywords:** Diabetes; Enzyme; Triazoles; ACE, *In silico*; DFT; Docking, simulation.**Correspondence:** \*Email: [abel.oyebamiji@bowen.edu.ng](mailto:abel.oyebamiji@bowen.edu.ng)

## Introduction

Globally, diabetes mellitus has been considered to be a severe condition since its discovery over two thousand years ago [1, 2]. Abnormal rise of blood sugar in human system remains one of the crucial issues battling man and woman all over the world [3]. Also, wrong release of insulin in human body system battling with diabetes results to risen level of blood sugar [4, 5]. According to Hosseini *et al.*, 2014, the activity of diabetes in human body system has led to many deaths and it has been ranked the third cause of death globally [6].

According to Zhao *et al.*, and Iwane *et al.* [7, 8], angiotensin converting enzyme (dipeptidyl carboxypeptidase with two isomers) was reported to be a very important target in patient with diabetes and this could be due to its ability to convert hypertensin I to form hypertensin II [7, 8]. The hydrophobic trans-membrane location together with minor cytoplasmic were observed to be situated in the isomers present in the studied target which were both found very close to human heart. [9] and this was reported by Hikmet *et al.*, to have capacity to regulate compression of human blood (i.e. blood pressure) [10]. More so, angiotensin converting enzyme indirectly heightens blood pressure of human beings which thereby brings about lessening of blood vessels and finally result to diabetes in human being [11]. It possesses Di isoform that could be converted within the same system and this has been observed to be present in diverse shapes in

numerous tissues. In some of the tissues present in angiotensin converting enzyme, such as somatic and human sperm cells, Di isoform could form glycoprotein. In somatic cell, N terminal and C terminal were present with different way of operation [12] and the active site located in both N and C-terminal catalyze the hydrolysis of angiotensin I with similar ability. Ehlers *et al.*, however revealed that the potential of N-terminal in blood pressure regulation proved to be decreased while C-terminal was confirmed to be energetic in regulating human blood pressure [13]. Therefore, the use of efficient drug-like agent to subdue angiotensin converting enzyme is extremely necessary.

The use of triazole and its derivatives in several fields such as agriculture, medicinal etc. has intrigued interest of many scientists and researchers around the globe. [14]. Widespread use of triazoles in numerous areas has been reported in many literatures to be due to their distinct configuration and features [15-17]. According to Zvenihorodska *et al.*, 2021, combination of heterocycles in a compound with series of derivatives makes promising situations for finding biological active substances [18]. Triazole and its chemistry was steadily established with numerous superficial and suitable synthetic procedures together with its useful biological relationship within the systems [19]. Therefore, this work is targeted at investigating the anti-angiotensin converting enzyme activity of the studied triazoles via

quantum chemical and molecular modeling studies using *in silico* approach.

## Materials and Method

### Quantum Chemical Study

The geometries of the studied triazoles derivatives were optimized at the DFT level. The density functional theory method employed in this study was implemented via three-parameter B3LYP density functional and as reported by Becke, 1993 [20], it includes Becke's gradient exchange correction as well as Lee, Yang, Parr correlation functional [21]. In this work, every calculation was performed by Spartan '14 program implemented on core i5 2.40 GHz and 2.50 GHz Computer. Molecular structure of the studied compounds obtained from the research work executed by Mohamed *et al.*, 2020 [22] were precisely sketched by making appropriate bond between suitable atoms. Using Spartan 14 software, the studied compounds were subjected to optimization using B3LYP and 6-31G\*\* as basis set [23]. The already optimized studied compounds which brought about lists of molecular descriptors that characterize the activities and properties of the studied compounds were obtained and reported. The geometries and features of the optimized compounds were observed before converting it to .pdb format for further study.

### Electronic descriptor-based QSAR model Analysis

Electronic features extracted from the investigated optimized triazole derivatives were further explored via quantitative structure activity

relationship (QSAR) study. The study was carried out using material studio software [24]. The optimized molecules were categorized into two (80%) for the training set and (20%) for the test set. The electronic-based features retrieved from the training set were used as the independent variable while the observed inhibition concentration (IC<sub>50</sub>) was set as dependent variable for developing QSAR model (equation 1). The validity of the QSAR model developed was determined via adjusted R<sup>2</sup> (equation 2).

$$IC_{50} = -2.40288 - 0.202787(E_{HOMO}) + 0.0389228(DM) - 0.00725026(PSA) + 1.45866(OVALITY) \text{-----(1)}$$

R<sup>2</sup>: 0.745234; Adjusted R<sup>2</sup>: 0.617852, P-value (F): 0.016771

$$R_a^2 = \frac{(N-1) \times R^2 - P}{N-1-P} \text{----- (2)}$$

### Molecular Docking Analysis

Potential inhibiting properties of the studied compounds (Supp. Table 1) against human angiotensin-converting enzyme (PDB ID: 3NXQ) [25] was explored using docking software [26-29]. The binding cavity of human angiotensin-converting enzyme was put into consideration and other deposits found in the binding cavity different from amino acid were removed. The appropriate procedure for protein preparation for docking was followed and finally saved as. pdbqt file. Size of the grid dimension was 30,30 and 30 for the (x,y and z dimension) and values obtained for the center in X = 1.097, Y = -15.572 and Z = -18.376 dimension were designated (Figure 1). Each docked complex was observed to have nine configurations. Autodock

was used in selecting superlative scoring position of each complex and Discovery Studio visualizer was employed for visualizing the interaction between the studied complexes.

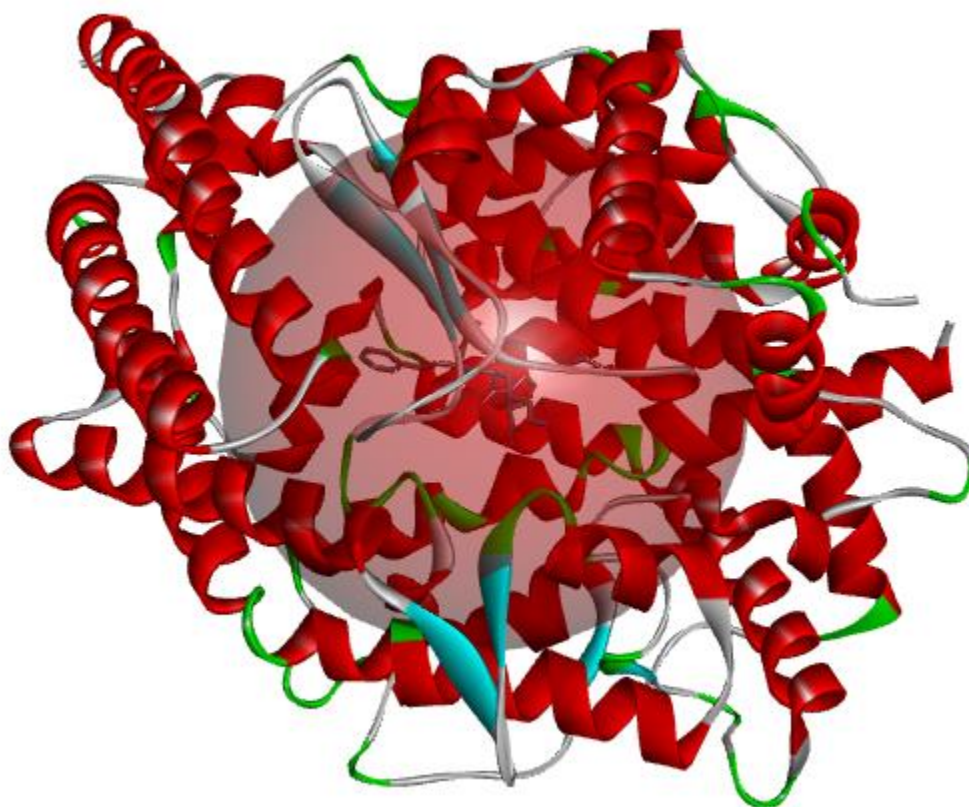


Figure 1: Studied receptor with identified binding site.

#### ***Molecular Dynamic Simulation (MDS) Study***

The calculation of binding energy and steadiness of compound 4-angiotensin converting enzyme complex as well as metformin--angiotensin converting enzyme complex were investigated using molecular dynamic simulation study with appropriate force field implanted in Gromacs software [30]. The steadiness via molecular dynamic simulation was reached using 100ns simulation time. The examined complex system was carried-out via TIP3P water molecule

in an orthorhombic box of 10 Å on all sides. Furthermore, suitable quantity of Chloride and Sodium ions was supplied to the system in order to counterbalance the charged system [31]. NVT and NPT ensemble were employed during the simulation for the sole purpose of implementing equilibration as well as achieving equilibration and minimization (using 100 nanoseconds with a 300 K and 1 bar) in the studied system respectively. More so, CPPTRAJ module was

used in analyzing molecular dynamics trajectories [32].

## Results and Discussion

### Calculated Ligand Features

The calculated optimized studied ligands brought about many ligands which exposed their potential reacting ability. The potential ability of any compound to relate well could be confirmed through its strength to donate electrons to other compounds within the appropriate range. Adeoye *et al.*, 2022 exposed that the greater the  $E_{\text{HOMO}}$  value, the better enhanced the level of reactivity of such compound; therefore, compound **4** showed the potential tendency to react well [33]. The calculated  $E_{\text{HOMO}}$  values are -4.84 e V, -5.19 e V, -5.20 e V, -4.53 e V, -5.09 e V, -5.19 e V, -5.04 e V, -4.87 e V, -5.17 e V, -5.47 e V, -5.22 e V, -5.12 e V, -5.26 e V, -5.55 e V, -5.31 e V for compound **1** to **15**. As shown in Table 1, it was observed that the presence of methyl and 2-ethyl-1H-indole as derivatives attached to the parent compound improved the donating ability of compound **4** thereby generating greater ability to offer electrons to the neighboring compounds. These derivatives also enhanced the reactivity of compound **4** which was observed through the calculated band gap for compound **4**. The energy gap for compound **1** to **15** were 4.00 e V, 4.30 e V, 4.35 e V, **3.73** e V, 4.23 e V, 4.38 e V, 3.90 e V, 4.08 e V, 4.27 e V, 4.49 e V, 4.26 e V, 4.27 e V, 4.43 e V, 4.91 e V and 4.52 e V. The electron donating capacity of the attached methyl in

compound **4** was observed to enhance the electron richness of compound **4** via carbon **2** and it is expected to have higher capability to attack electrophilic sites than other investigated triazole derivatives (figure 2).

Also, the calculated  $E_{\text{LUMO}}$  were -0.84 e V for compound **1**, -0.89 e V for compound **2**, -0.85 e V for compound **3**, -0.80 e V for compound **4**, -0.86 e V for compound **5**, -0.81 e V for compound **6**, **-1.14** e V for compound **7**, -0.79 e V for compound **8**, -0.90 e V for compound **9**, -0.98 e V for compound **10**, -0.96 e V for compound **11**, -0.85 e V for compound **12**, -0.83 e V for compound **13**, -0.64 e V for compound **14**, -0.79 e V for compound **15**. Compound **7** with lowest  $E_{\text{LUMO}}$  value revealed that it has the greatest strength to accept electrons from any compound with capacity to release electrons. The capability of compound **7** to receive electrons is a function of the attached derivatives (Hydrogen and 5-ethyl-1H-imidazole) to the parent compound. Also, the lower the energy gap value, the better the interaction between two molecules; thus, compound **4** showed that it has higher strength to react well than other studied ligands. As shown in table 2, it was revealed that the calculated lipophilicity (Log P) for compound 1-15 was observed to be lower than 5 which showed the studied compounds have ability to act as drug-like agent. Other predicted features retrieved from the optimized molecules were presented in table 2.

Table 2: 3-dimensional based descriptors from examined optimized Triazole derivatives

	$E_{\text{HOMO}}$	$E_{\text{LUMO}}$	EG	DM	MW	AREA	VOL	PSA	OVA	LOG P
--	-------------------	-------------------	----	----	----	------	-----	-----	-----	-------

1	-4.84	-0.84	4.00	8.21	404.447	401.07	374.71	119.155	1.60	0.15
2	-5.19	-0.89	4.30	3.91	418.474	410.17	391.97	115.999	1.58	0.51
3	-5.20	-0.85	4.35	6.91	519.582	515.31	491.55	132.337	1.71	-0.38
4	-4.53	-0.80	3.73	9.42	533.609	523.31	508.70	127.212	1.70	-0.02
5	-5.09	-0.86	4.23	5.31	432.501	438.88	412.08	121.402	1.64	1.04
6	-5.19	-0.81	4.38	4.65	446.528	444.18	428.01	114.198	1.62	1.39
7	-5.04	-1.14	3.90	3.44	470.510	457.87	433.20	135.633	1.65	-1.04
8	-4.87	-0.79	4.08	5.60	480.545	481.81	459.42	115.520	1.67	1.03
9	-5.17	-0.90	4.27	2.96	426.497	411.97	406.12	80.055	1.55	1.77
10	-5.47	-0.98	4.49	3.27	460.942	427.66	419.40	88.055	1.58	1.63
11	-5.22	-0.96	4.26	2.54	444.487	417.60	410.74	79.862	1.56	1.23
12	-5.12	-0.85	4.27	2.75	456.523	441.64	433.22	86.974	1.60	0.79
13	-5.26	-0.83	4.43	0.44	404.491	387.82	382.86	80.496	1.52	1.91
14	-5.55	-0.64	4.91	3.01	418.518	403.33	400.67	84.872	1.53	2.33
15	-5.31	-0.79	4.52	1.86	432.545	419.39	417.57	82.514	1.55	2.75

Note: "EG: Energy gap; DM: dipole moment; MW: molecular weight; Vol: Volume; PSA: polar surface area; Ova: Ovality; LogP: Lipophilicity".

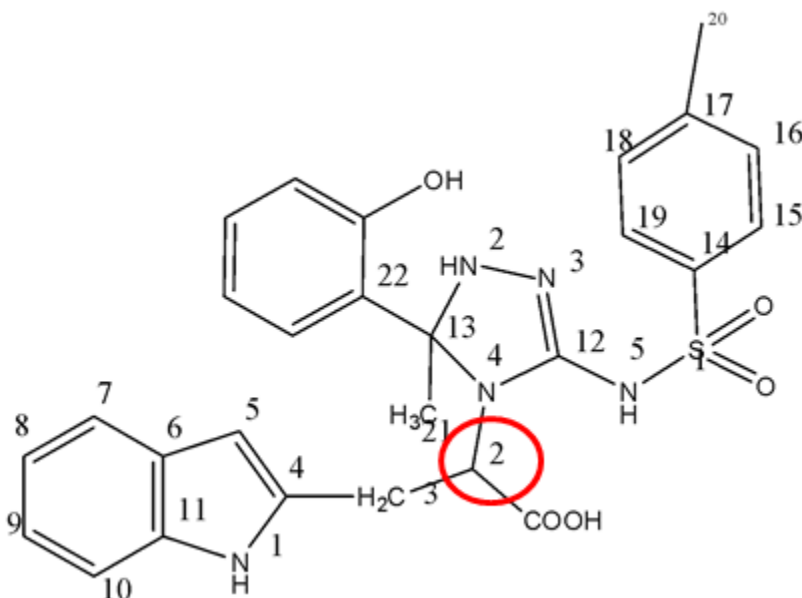


Figure 2: 2D structure of compound 4

### Molecular Docking Study

The potential inhibiting ability of the examined triazoles were investigated against



angiotensin converting enzymes (PDB code: 3NXQ). This investigation was achieved with docking study; employing the use of several software such as discovery studio, pymol, autodock tool and autodock vina. The biochemical relationship exhibited between the studied chemical compounds and angiotensin converting enzyme (PDB code: 3NXQ) were examined and reported. Table 3 revealed the calculated scoring, the amino acid residues responsible for the interaction that is been investigated as well as type of the non-bonding interaction occurring between the examined complexes and the residues of amino acid. The scoring was calculated in kcal/mol and the calculated value for individual docked complex were -8.7 for compound **1**, -8.7 for compound **2**, -10.2 for compound **3**, -10.5 for compound **4**, -9.0 for compound **5**, -9.1 for compound **6**, -9.6 for compound **7**, -9.1 for compound **8**, -9.3 for compound **9**, -9.1 for compound **10**, -9.1 for compound **11**, -8.7 for compound **12**, -8.4 for compound **13**, -8.8 for compound **14**, and 9.0 for

compound **15**. Report by Ibrahim *et al.*, 2023 revealed that lowest calculated scoring value is expected to bind better, as indicated in table 3, it was detected that compound **4** with -10.5 kcal/mol was the compound with lowest binding affinity and possess potential ability to inhibit angiotensin converting enzyme (PDB code: 3NXQ) than other investigated triazole derivatives as well as the Metformin (Reference drug) [34, 35]. The efficiency of Compound **4** was observed to be the function of the methyl and 2-ethyl-1H-indole attached to the parent compound in compound **4** which was observed to enhance the electron richness of compound **4** via carbon 2 thereby improving the biological/inhibiting activity of compound **4** against angiotensin converting enzyme (PDB code: 3NXQ) (Figure 3). More so, the observed residues of amino acid and the nature of non-bonding interaction observed on the active site of the studied target during docking were reported in Supp Figure 1-3, 5-15.

Table 3: Scoring calculated in kcal/mol

	Binding Affinity (kcal/mol)	Amino Acid Residues
<b>1</b>	-8.7	Thr358, Gln355, Asp354, Arg350, Glu262, Ser260, Tyr501, Phe505, Phe435, Gln259, Lys489
<b>2</b>	-8.7	His491, His331, Gln259, Leu139
<b>3</b>	-10.2	Glu431, Asp354, Thr358, Met256, Thr144, Trp257, Asp255, His361, Gln355, Arg350
<b>4</b>	-10.5	Asp354, His491, Gln355, Tyr 501, Phe505, Gln259, Lys489, Trp257, His331
<b>5</b>	-9.0	Cys330, His331, Tyr501, His361, Gln259, Lys489

<b>6</b>	-9.1	Phe505, Tyr501, Phe435, Trp257, Ser260, Arg350, Thr358
<b>7</b>	-9.6	Gln355, Thr358, Asp255, Thr144, Gln259, Tyr501, Phe435, Phe505
<b>8</b>	-9.1	Arg350, Gln355, Trp257, Thr358, Glu362, His361, Lys489, His331
<b>9</b>	-9.3	Tyr501, Asp255, Gln355
<b>10</b>	-9.1	Thr358, His331, Gln259, Lys432, Glu262, Ser357
<b>11</b>	-9.1	Trp257, Asp255, Gln259, His491, Tyr501, Thr358, Arg350
<b>12</b>	-8.7	His361, Thr358, Arg350, His331
<b>13</b>	-8.4	Phe 435, Asp354, Thr358, Gln355
<b>14</b>	-8.8	Asp255, Trp257, Thr358, Gln355
<b>15</b>	-9.0	Phe505, Gln259, His491, His331, Ala332
<b>ref</b>	-5.6	-

*Ref: Metformin*



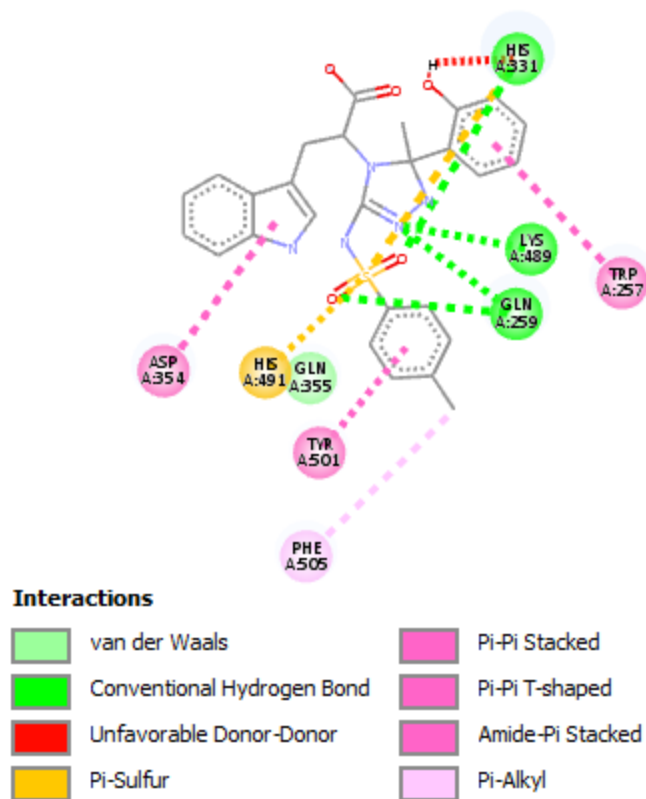


Figure 3: Two-dimensional structure of compound 4 in active site of the target

### ***Quantitative Structure Activities Relationship Study***

The Quantitative Structure Activities Relationship model developed was obtained using genetic function algorithm (GFA) via Material Studio 2017 software [36]. The set of descriptors generated from the studied compounds after optimization were used for this investigation. The 20% training set were screened and the molecular descriptor used for developing the model were highest occupied molecular orbital, dipole moment, polar surface area and ovality. As shown in table 4, the predicted percentage inhibition concentration for each of the compounds for the training set was closer to

the exact value for the observed inhibition concentration (Figure 4). The predicted result obtained showed the proficiency of the developed model which was confirmed via the squared correlation coefficient ( $R^2$ ). The developed model was further validated so as to certify the validity and reliability of the model. The factors that were put into consideration for the validation were adjusted squared correlation coefficient (Adjusted  $R^2$ ) and P-value. Furthermore, the reliability and validity of the QSAR developed model was subjected to further confirmation via test set and it was observed that the predicted inhibition concentration (% $IC_{50}$ ) for the test set was closer to observed % $IC_{50}$  for the test set

which was established via the calculated residual value.

More so, the plot of residual values against observed %IC<sub>50</sub> revealed the level of undifferentiated widening of the residual values on both sides of the horizontal lines and this also

depicts the accuracy and level of dependency of the developed QSAR model (Figure 5). The coefficient, standard error, t-ratio and p-value for the variables in the developed QSAR model were shown in table 5.

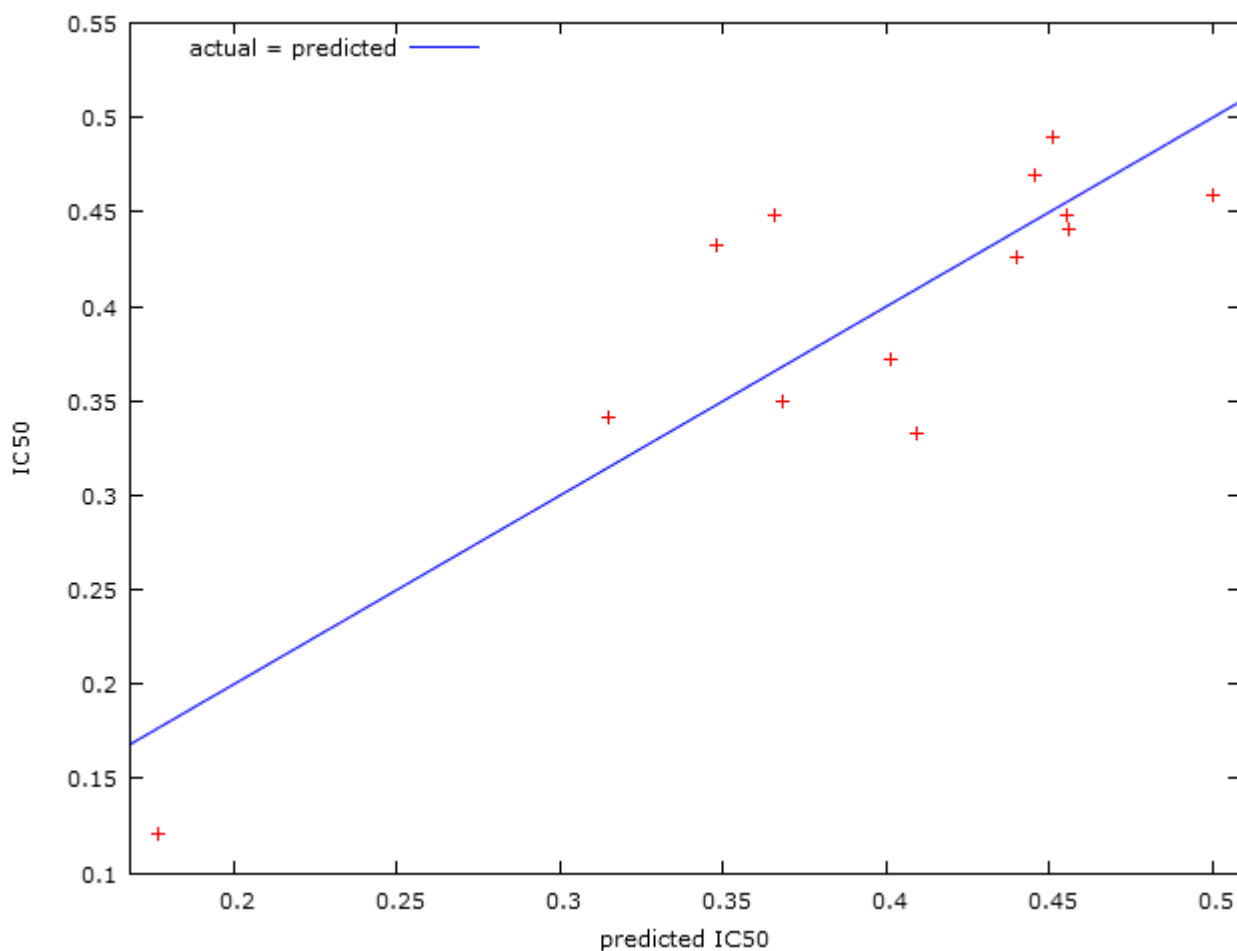
Table 4: Observed and predicted %IC<sub>50</sub> for studied Triazoles

	<b>Observed %IC<sub>50</sub></b>	<b>Fitted %IC<sub>50</sub></b>	<b>residual</b>
<b>1</b>	0.350	0.368	-0.018
<b>2*</b>	0.410	0.265	0.145
<b>3</b>	0.448	0.455	-0.007
<b>4</b>	0.426	0.440	-0.014
<b>5</b>	0.432	0.348	0.084
<b>6</b>	0.448	0.366	0.082
<b>7</b>	0.121	0.176	-0.055
<b>8</b>	0.372	0.401	-0.029
<b>9*</b>	0.428	0.441	-0.013
<b>10</b>	0.459	0.500	-0.041
<b>11</b>	0.490	0.451	0.039
<b>12</b>	0.470	0.446	0.024
<b>13</b>	0.341	0.314	0.027
<b>14</b>	0.441	0.456	-0.015
<b>15</b>	0.333	0.409	-0.076

\* denotes test set

Table 5: Calculated coefficient, standard error, t-ratio and p-value for the QSAR model variables

	<b>coefficient</b>	<b>std. error</b>	<b>t-ratio</b>	<b>p-value</b>	
<b>const</b>	-2.40288	1.10949	-2.166	0.0622	*
<b>E<sub>HOMO</sub></b>	-0.202787	0.0983777	-2.061	0.0732	*
<b>DM</b>	0.0389228	0.0123778	3.145	0.0137	**
<b>PSA</b>	-0.00725026	0.00176235	-4.114	0.0034	***
<b>OVALITY</b>	1.45866	0.636422	2.292	0.0511	*

Figure 4: Plot of observed IC<sub>50</sub> against predicted IC<sub>50</sub>

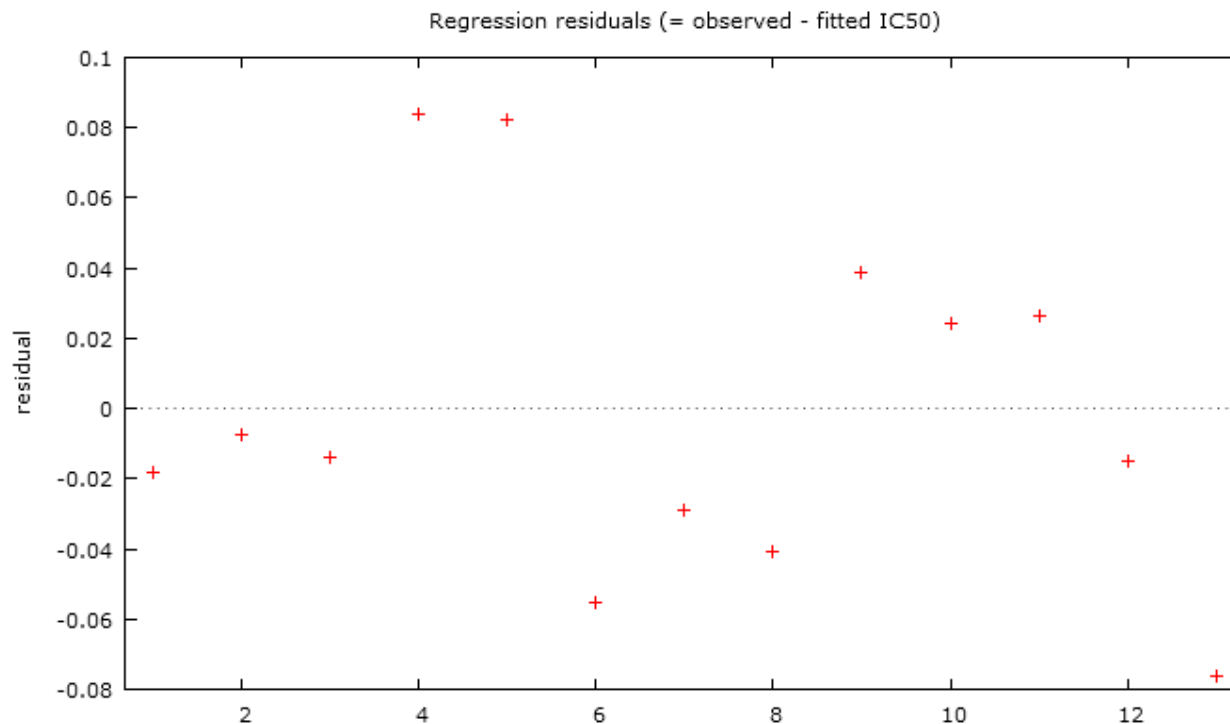


Figure 5: Plot of residual value against observed %IC<sub>50</sub>

### Pharmacokinetics Study

Pharmacokinetics study was carried out using ADMETSAR1 software [34] on compound 4 and Metformin. Compound 4 was considered for this investigation due to high binding affinity and its better inhibiting capability and the pharmacokinetic report was displayed in table 6. The factors put into consideration for this study were presented in Supplementary tables 2 and 3. As shown in Supplementary tables 2 and 3, the values calculated for the factors put into consideration for compound 4 and referenced drug were closer and this showed that they have similar drug-like features.

### 3.4. Molecular Dynamic Simulation Analysis

#### Root Mean Square Deviation (RMSD)

The level of deviation from the preliminary configuration as well as the stability of Compound 4-angiotensin converting enzyme complex and metformin- angiotensin converting enzyme complex via 100ns was investigated via root mean square deviation analysis. As shown in figure 6, the RMSD of 2-(5-(2-hydroxyphenyl)-5-methyl-3-(4-methylphenylsulfonamido)-1H-1,2,4-triazol-4(5H)-yl)-3-(1H-indol-3-yl)propanoic acid (Compound 4)-angiotensin converting enzyme complex proved to be more stable than the RMSD of metformin- angiotensin converting enzyme complex and this showed that compound 4 fairly related with the investigated target thereby inhibited the target than the Metformin.

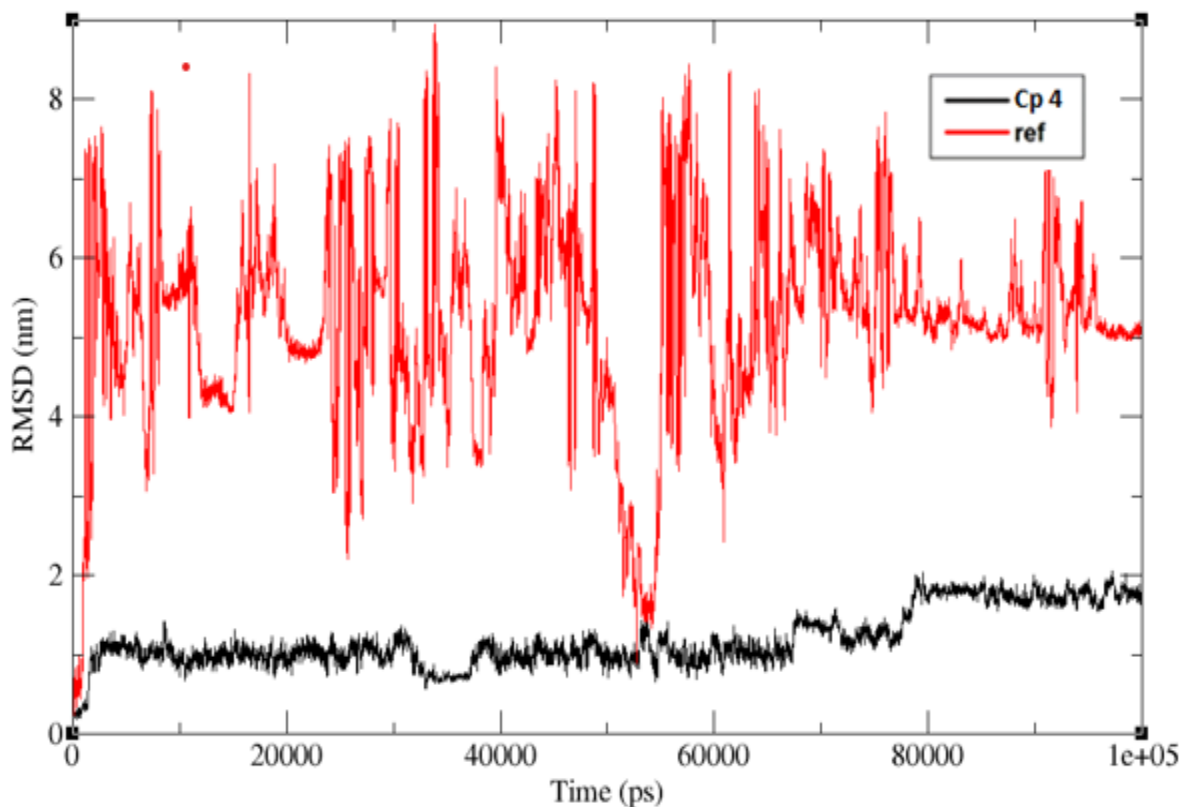


Figure 6: RMSD of Compound 4-ace and metformin-ace complexes during 100ns simulation

### Calculated Binding Energy

The simulation of Compound 4-angiotensin converting enzyme complex and metformin-angiotensin converting enzyme complex which brought about series of binding components were accomplished via molecular dynamic simulation study. As shown in table 8, the calculated binding energy components were  $\Delta E_{vdw}$  ( $-22.63 \pm 0.91$  for comp4-ACE complex;  $-8.55 \pm 0.49$  for Ref-ACE complex),  $\Delta E_{ele}$  ( $-55.88 \pm 2.37$  for comp4-ACE ;  $-11.1 \pm 1.8$  for Ref-ACE complex),  $\Delta G_{gas}$  ( $-78.51 \pm 1.64$  for comp4-ACE complex;  $-19.65 \pm 1.76$  for Ref-ACE complex),  $\Delta G_{sol}$  ( $78.89 \pm 0.83$  for comp4-

ACE complex;  $25.5 \pm 1.19$  for Ref-ACE complex), and  $\Delta G_{bind}$  ( $0.38 \pm 1.0$  for comp4-ACE complex;  $5.85 \pm 1.1$  for Ref-ACE complex) (Figures 7 and 8). The calculated value for van der Waal energy, electrostatic energy and gas-phase components were more favorable towards inhibiting the ability of compound 4 against angiotensin converting enzyme than the referenced compound against angiotensin converting enzyme. According to the report by Oyebamiji *et al.*, 2020 [37], the lower the binding free energy of a compound, the better the capacity of such compound to interact and inhibit the target; thus, compound 4 with 0.38 kcal/mol

proved to be a potential anti- angiotensin converting enzyme agent than metformin.

**Table 8: Binding Energy Components**

Complexes	Binding Energy Components (kcal/mol)				
	$\Delta E_{vdw}$	$\Delta E_{ele}$	$\Delta G_{gas}$	$\Delta G_{sol}$	$\Delta G_{bind}$
<b>Comp4-ACE</b>	$-22.63 \pm 0.91$	$-55.88 \pm 2.37$	$-78.51 \pm 1.64$	$78.89 \pm 0.83$	$0.38 \pm 1.0$
<b>REF-ACE</b>	$-8.55 \pm 0.49$	$-11.1 \pm 1.8$	$-19.65 \pm 1.76$	$25.5 \pm 1.19$	$5.85 \pm 1.1$

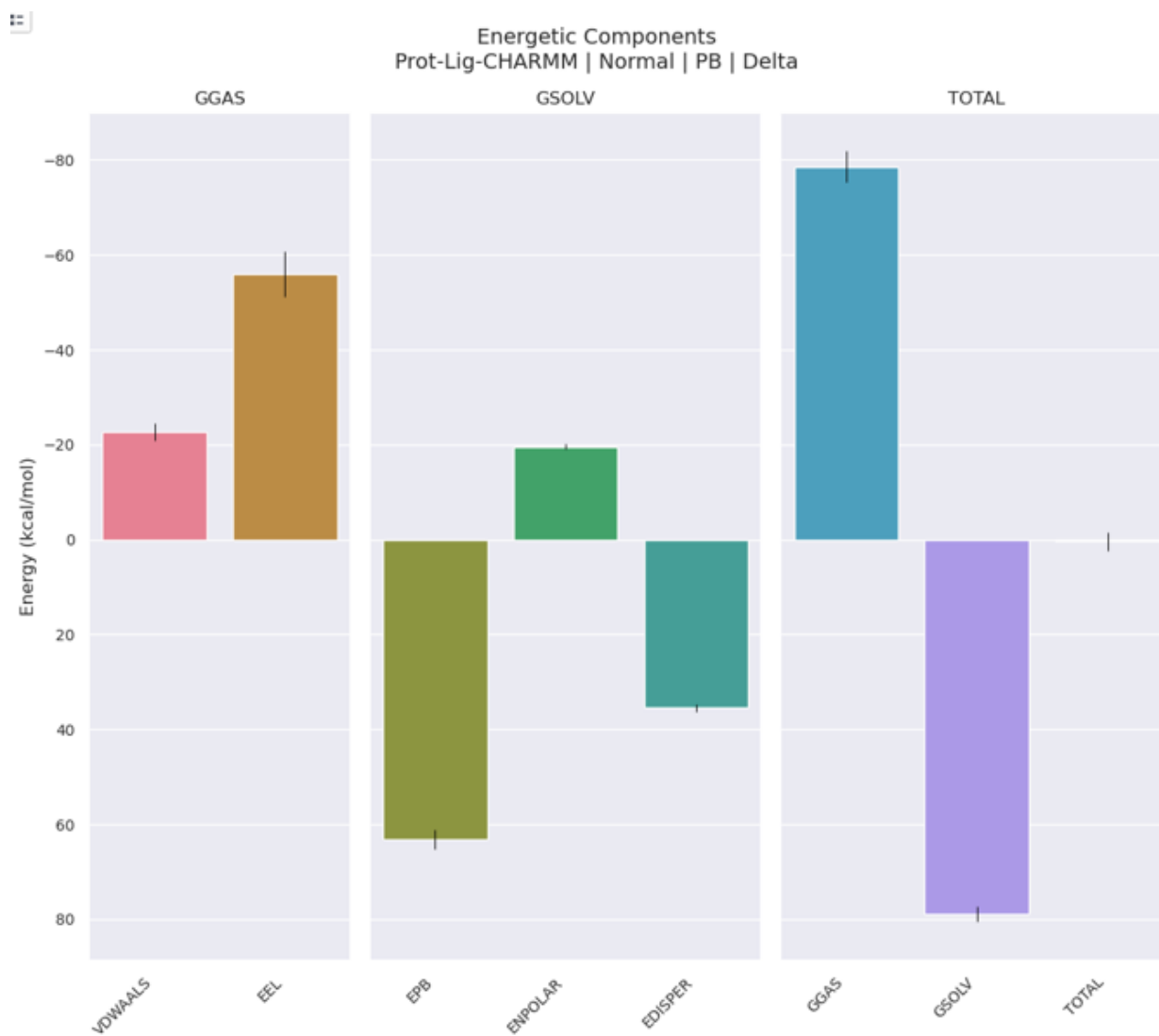




Figure 7: Chart showing the calculated energetic components for Comp4-ACE complex

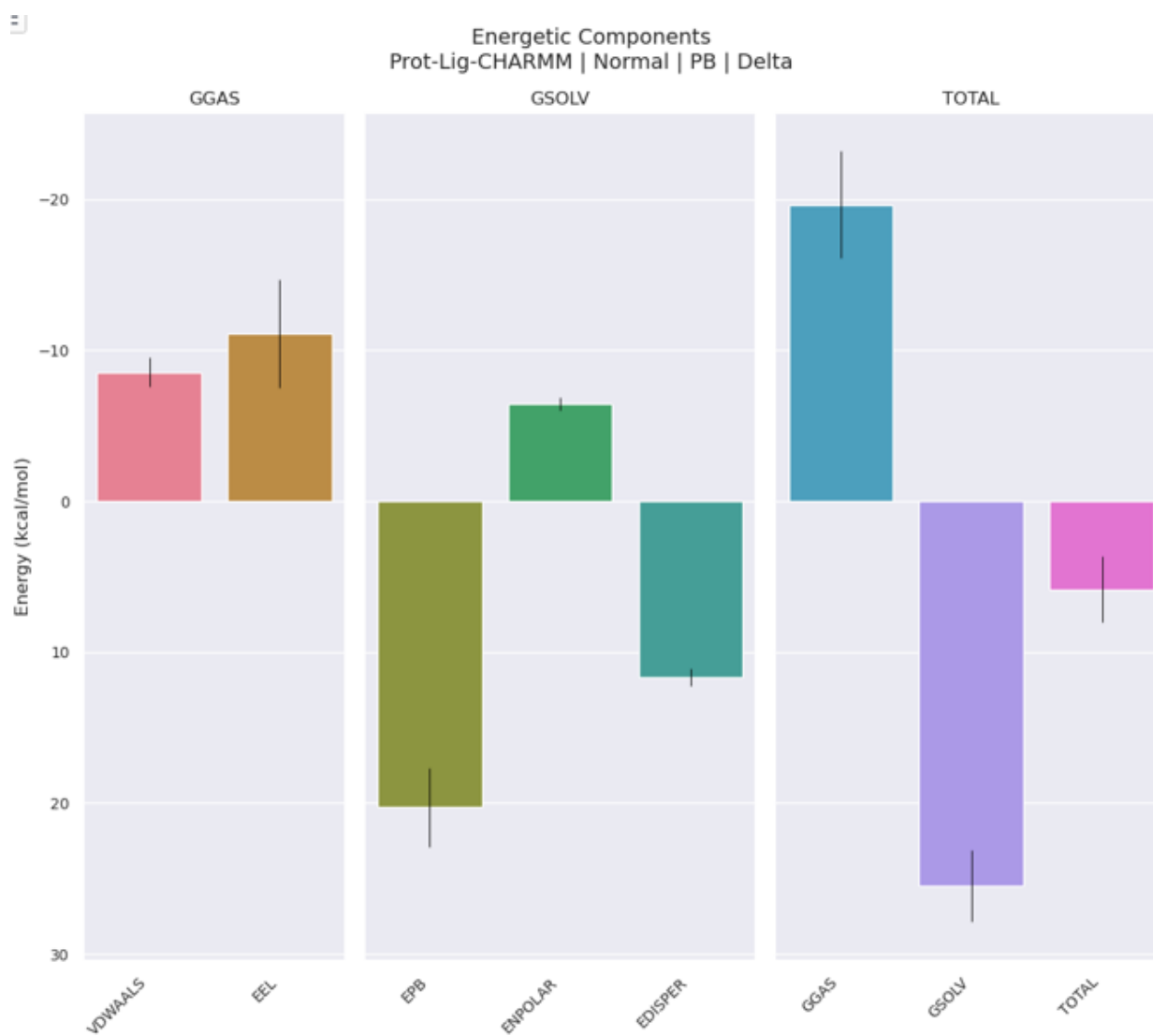


Figure 8: Chart showing the calculated energetic components for Ref-ACE complex

## Conclusion

The use of integrated approach was employed to investigate the biological activities of triazole derivatives. Fifteen triazole-based compounds were optimized using Spartan 14

software with 6-31G\*\* as a basis set. Highest occupied molecular orbital energy ( $E_{HOMO}$ ) and band gap ( $E_{LUMO} - E_{HOMO}$ ) were discovered to play a pivotal in the activity of compound **4** which thereby improved its inhibiting activity against

angiotensin converting enzyme (PDB ID: 3NXQ) than other studied compounds as well as the reference drug (metformin). Further confirmation was carried out to ascertain the effective inhibiting activity of compound **4** against angiotensin converting enzyme (PDB ID: 3NXQ) via molecular dynamic simulation, the pharmacokinetic properties of compound **4** were compared to the features obtained for metformin and it was observed that Compound **4** has the capability to be a potential anti-diabetic agent.

### References

- [1]. Latha S., Vijayakumar R. (2019). The Facts about Diabetes Mellitus- A Review. *Galore International Journal of Health Sciences and Research*; 4(2).
- [2]. Lakić B., Škrbić R., Uletilović S., Mandić-Kovačević N., Grabež M., Šarić M. P., Stojiljković M. P., Soldatović I., Janjetović Z., Stokanović A., Stojaković N., Mikov M. (2024). Beneficial Effects of Ursodeoxycholic Acid on Metabolic Parameters and Oxidative Stress in Patients with Type 2 Diabetes Mellitus: A Randomized Double-Blind, Placebo-Controlled Clinical Study, *Journal of Diabetes Research*, 2024, Article ID 4187796, 10 pages, 2024. <https://doi.org/10.1155/2024/4187796>
- [3]. Oyebamiji A.K, Soetan E.A, Akintelu S.A., Ayeleso A.O, Mukwevho E. (2022). Alpha-glucosidase activity of phytochemicals from *Phyllanthus amarus* leaves via *in-silico* approaches. *Pharmacological Research - Modern Chinese Medicine* 2: 100054. <https://doi.org/10.1016/j.prmcm.2022.100054>
- [4]. Missoun F., Bouabdelli F., Baghdad A, Amari N, Djebli N. (2018). Antidiabetic bioactive compounds from plants, *Med. Technol. J.* 2(2): 199–214 . [10.26415/2572-004X-vol2iss1p199-214](https://doi.org/10.26415/2572-004X-vol2iss1p199-214)
- [5]. Zheng W., Ji X., Yin Q. q., Wu C., Xu C., Pan H., Wu C. (2024). Exosomes as Emerging Regulators of Immune Responses in Type 2 Diabetes Mellitus, *Journal of Diabetes Research*, Article ID 3759339, 9 pages. <https://doi.org/10.1155/2024/3759339>
- [6]. Hosseini S, Huseini HF, Larijani B, Mohammad K, Najmizadeh A, Nourijelyani K, Jamshidi L. (2014). The hypoglycemic effect of Juglans regia leaves aqueous extract in diabetic patients: a first human trial, *DARU J. Pharm. Sci.* 22: 19. [10.1186/2008-2231-22-19](https://doi.org/10.1186/2008-2231-22-19)
- [7]. Zhao BW, Chen YJ, Zhang RP, Chen YM, Huang BW. (2024). Angiotensin-converting enzyme 2 alleviates liver fibrosis through the renin-angiotensin system. *World J Gastroenterol.* 30(6): 607-609 [DOI: 10.3748/wjg.v30.i6.607]
- [8]. Iwane S., Nemoto W., Miyamoto T. et al. (2024). Clinical and preclinical

- evidence that angiotensin-converting enzyme inhibitors and angiotensin receptor blockers prevent diabetic peripheral neuropathy. *Sci Rep* 14, 1039. <https://doi.org/10.1038/s41598-024-51572-z>
- [9]. Bellomo R., Zarbock A. & Landoni G. (2024). Angiotensin II. *Intensive Care Med* 50, 279–282 <https://doi.org/10.1007/s00134-023-07290-7>
- [10]. Hikmet F., Méar L., Edvinsson Å, Micke P, Uhlén M. Lindskog, C. (2020). The protein expression profile of ACE2 in human tissues, *Mol. Syst. Biol.* 16 (7): e9610. doi: 10.15252/msb.20209610.
- [11]. Alabsi S., Dhole A., Hozayen S., Chapman S.A. (2023). Angiotensin-Converting Enzyme 2 Expression and Severity of SARS-CoV-2 Infection. *Microorganisms*, 11, 612. <https://doi.org/10.3390/microorganisms11030612>
- [12]. Golcuk M., Yildiz A., Gur M. (2022). Omicron BA.1 and BA.2 Variants Increase the Interactions of SARS-CoV-2 Spike Glycoprotein with ACE2. *J. Mol. Graph. Model.* 117, 108286.
- [13]. Beyerstedt, S.; Casaro, E.B.; Rangel, É.B. COVID-19: Angiotensin-Converting Enzyme 2 (ACE2) Expression and Tissue Susceptibility to SARS-CoV-2 Infection. *Eur. J. Clin. Microbiol. Infect. Dis. Off. Publ. Eur. Soc. Clin. Microbiol.* 2021, 40, 905–919
- [14]. Zahra K, Mahrokh M, Abolfazl S, Seyed AK, Mojtaba F, and Elham Z. (2022). Novel 1, 2, 4-Triazoles as Antifungal Agents. *BioMed Research International*, Article ID 4584846, 39 pages. doi: [10.1155/2022/4584846](https://doi.org/10.1155/2022/4584846)
- [15]. Vaishnani M.J., Bijani S., Rahamathulla M., Baldaniya L., Jain V., Thajudeen K.Y., M. Ahmed M., Farhana S.A. & Pasha I. (2024) Biological importance and synthesis of 1,2,3-triazole derivatives: a review, *Green Chemistry Letters and Reviews*, 17, 1, DOI: [10.1080/17518253.2024.2307989](https://doi.org/10.1080/17518253.2024.2307989)
- [16]. Mekheimer R.A., Abuo-Rahma G.E.D.A., Abd-Elmonem M., Yahia R., Hisham M., Hayallah A.M., Mostafa S.M., Abo-Elsoud F.A., Sadek K.U. (2022). New S-Triazine/Tetrazole Conjugates as Potent Antifungal and Antibacterial Agents: Design, Molecular Docking and Mechanistic Study. *J. Mol. Struct.* 1267, 133615. doi:10.1016/j.molstruc.2022.133615.
- [17]. Kabir E., Uzzaman M. (2022). A Review on Biological and Medicinal Impact of Heterocyclic Compounds. *Results. Chem.* 4 (8), 100606. doi:10.1016/j.rechem.2022.100606.

- [18]. Zvenihorodska T, Hotsulia A, Kravchenko S, Fedotov S, Kyrychko B. (2021). Synthesis and Antimicrobial Action of 1,2,4-Triazole Derivatives Containing Theophylline and 1,3,4-Thiadiazole Fragments In their Structure. *Afr. J. Biomed. Res.* 24: 159- 163
- [19]. Matin M.M, Matin P, Rahman M.R, Ben Hadda T, Almalki F.A, Mahmud S, Ghoneim M.M, Alruwaily M, and Alshehri S. (2022). Triazoles and Their Derivatives: Chemistry, Synthesis, and Therapeutic Applications. *Front. Mol. Biosci.* 9: 864286. <https://doi.org/10.3389/fmolb.2022.864286>
- [20]. Becke A.D., (1993). Density-functional thermochemistry. III. The role of exact exchange, *J. Chem. Phys.* 1993, 98, 5648-5652.
- [21]. Lee C., Yang W., and Parr R.G., (1988). Development of the Colle-Salvetti correlation-energy formula into a functional of the electron density. *Phys. Rev. B*, 37, 785-789.
- [22]. Mohamed M.A.A, Abd Allah O.A, Bekhit, A.A, Kadry A.M, El-Saghier AMM. (2020). Synthesis and antidiabetic activity of novel triazole derivatives containing amino acids. *J Heterocyclic Chem.* 57: 2365–2378. <https://doi.org/10.1002/jhet.3951>
- [23]. Oyebamiji A.K., Akintelu S.A, Akande I.O, Aworinde, H.O, Adepegba O.A, Akintayo E.T, Akintayo C.O., Semire B., Babalola J.O. (2023). Dataset on biochemical inhibiting activities of selected phytochemicals in *Azadirachta indica L* as potential NS2B–NS3 proteases inhibitors. *Data in Brief*, 48: 109162. <https://doi.org/10.1016/j.dib.2023.109162>
- [24]. Oyebamiji A.K, Fadare O.A, and Semire B. (2020). Hybrid-based drug design of 1,2,3-triazolepyrimidine-hybrid derivatives: Efficient inhibiting agents of mesenchymal–epithelial transition factor reducing gastric cancer cell growth. *Journal of Chemical Research*, 44(5-6): 277–280. <https://doi.org/10.1177/174751981989833>
- [25]. Anthony C.S, Corradi H.R, Schwager S.L, Redelinghuys P, Georgiadis D, Dive V, Acharya K.R, Sturrock E.D. (2010). The N domain of human angiotensin-I-converting enzyme: the role of N-glycosylation and the crystal structure in complex with an N domain-specific phosphinic inhibitor, RXP407. *J Biol Chem* 285: 35685-35693. doi: 10.1074/jbc.M110.167866.
- [26]. Semire B, Oyebamiji A.K, and Odunola O.A. (2020). Electronic Properties’ Modulation of D-A-A via Fluorination

- of 2-Cyano-2-pyran-4-ylidene-Acetic Acid Acceptor Unit for Efficient DSSCs: DFT-TDDFT Approach. *Scientific African*, 7: e00287. <https://doi.org/10.1016/j.sciaf.2020.e00287>.
- [27]. Abdul-Hammed M, Semire B, Adegboyega S.A, Oyebamiji A.K, and Olowolafe T.A. (2020). Inhibition of Cyclooxygenase-2 and Thymidylate Synthase by Dietary Sphingomyelins: Insights from DFT and Molecular Docking Studies. *Phys. Chem. Res.*, 8(2): 296-310. [10.22036/PCR.2020.214026.1717](https://doi.org/10.22036/PCR.2020.214026.1717)
- [28]. Oyewole R.O, Oyebamiji, A.K.; Semire, B. (2020). Theoretical calculations of molecular descriptors for anticancer activities of 1, 2,3-triazole-pyrimidine derivatives against gastric cancer cell line (MGC-803): DFT, QSAR and docking approaches. *Heliyon*, 6: e03926. <https://doi.org/10.1016/j.heliyon.2020.e03926>
- [29]. Adegoke R.O., Oyebamiji A.K., and Semire B. (2020). Dataset on the DFT-QSAR, and docking approaches for anticancer activities of 1, 2, 3-triazole-pyrimidine derivatives against Human Esophageal Carcinoma (EC-109), *Data in Brief*, 31: 105963. doi: [10.1016/j.dib.2020.105963](https://doi.org/10.1016/j.dib.2020.105963)
- [30]. Çevik U.A, Celik I, Işık A, Pillai R.R., Tallei, T.E, Yadav R, Özkay Y, Kaplancıklı Z.A. (2022). Synthesis, molecular modeling, quantum mechanical calculations and ADME estimation studies of benzimidazole-oxadiazole derivatives as potent antifungal agents. *J. Mol. Struct.* 1252: 132095. <https://doi.org/10.1016/j.molstruc.2021.132095>
- [31]. Ahmad I., Akand S.R., Shaikh M, Pawara R, Manjula S.N, Patel H. (2022). Design, synthesis, in vitro anticancer and antimicrobial evaluation, SAR analysis, molecular docking and dynamic simulation of new pyrazoles, triazoles and pyridazines based isoxazole. *J. Mol. Struct.* 1251: 131972. <https://doi.org/10.1016/j.molstruc.2022.133312>
- [32]. Roe D.R, and Cheatham III T.E. (2013). PTRAJ and CPPTRAJ: software for processing and analysis of molecular dynamics trajectory data, *Journal of Chemical theory and Computation*, 9(7): 3084–3095. <https://doi.org/10.1021/ct400341p>
- [33]. Adeoye M.D., Oyebamiji A.K, Ashiru M.A, Adigun R.A, Olalere O.H, Semire B. (2022). Biological evaluation of selected metronidazole derivatives as anti-nitroreductase via in silico approach. *Eclética Química Journal*,

- 47(4): 27-36. DOI:[10.26850/1678-4618eqj.v47.4.2022.p27-36](https://doi.org/10.26850/1678-4618eqj.v47.4.2022.p27-36)
- [34]. Omotayo I.A, Semire B, Oladuji T.E., Latona D.F., Oyebamiji A.K., Owonikoko A.D., Abdulsalami I.O., Adeoye M.D., and Odunola, O.A. (2023). Molecular properties and In silico bioactivity evaluation of (4-fluorophenyl)[5]-3-phen-(4-nitrophenyl-4,5-dihydro-1H-pyrazol-1-yl)methanone derivatives: DFT and molecular docking approaches. *Journal of Taibah University Medical Sciences*, 18(6): 1386-1405. <https://doi.org/10.1016/j.jtumed.2023.05.011>.
- [35]. Oyebamiji A.K, Akintayo E.T., Akintayo C.O., Aworinde H.O., Adekunle O.D., Akintelu S.A. (2023). Cyclic RGD-containing peptides: in silico exploration against BCL-X(L). *Ukr. Biochem. J.* 95(2): 93-105. DOI: 10.15407/ubj95.02.093
- [36]. Oyebamiji A.K., Fadare, O.A., Semire, B. (2020). Anti-gastric cancer activity of 1,2,3-triazolo[4,5-d]pyrimidine hybrids (1,2,3-TPH): QSAR and molecular docking approaches. *Heliyon*, 6: e03561. doi: 10.1016/j.heliyon.2020.e03561
- [37]. Oyebamiji A.K., Tolufashe G.F., Oyawoye O.M., Oyedepo T.A., and Semire B. (2020). Biological Activity of Selected Compounds from *Annona muricata* Seed as Antibreast Cancer Agents: Theoretical Study. *Journal of Chemistry*, Article ID 6735232, 10 pages. <https://doi.org/10.1155/2020/6735232>